

Molecular Dynamics Simulation of Polymer Fine Particles. Physical and Mechanical Properties[†]

Kazuhiko FUKUI, Bobby G. SUMPTER, Michael D. BARNES, and Donald W. NOID

*Chemical and Analytical Sciences Division, Oak Ridge National Laboratory,
Oak Ridge, TN 37831-6197, U.S.A.*

(Received February 15, 1999)

ABSTRACT: Molecular dynamics simulations are used to study the atomistic details of nanometer scale polyethylene (PE) particles to gain insight into the properties and behavior of ultra fine polymer powders. From the nano-sized particles generated with up to 60000 atoms using an efficient MD method, structure and a variety of structural and physical characteristics were computed by averaging over sets of microstates at particular temperatures. The melting point, glass transition temperature, and heat capacity of the particles as a function of polymer chain length and particle size were obtained by monitoring the molecular volume and total energy. The results of our simulations predict an interesting reduction of the melting point and significantly smaller compressive modulus in comparison with the bulk system.

KEY WORDS Molecular Dynamics / Polymer Particles / Melting Point / Compressive Modulus / Polyethylene /

Ultra fine particles have received a great deal of attention in the ceramics and metallurgy literature due to their novel properties. These property abnormalities are due to the tremendous size reduction where critical length scales of physical phenomena become comparable to or larger than the size of the entire structure. Applications of such particles take advantage of high surface area and confinement effects, which lead to nanostructures with different properties than conventional materials. An example of the dependence of physical properties on the size is the melting point for gold which decreases dramatically as the size decreases.¹ One of the major reasons for this phenomenon is the large of amount of surface area and hence reduction of the nonbonded interactions for the surface layer. Clearly, such changes offer extraordinary potential for development of new materials in the form of bulk, composites and blends which can be used for coatings, optoelectronic components, magnetic media, ceramics and special metals, micro or nano-manufacturing, and bioengineering.²

Recently an experimental technique was developed at ORNL for creating very fine polymer particles of arbitrary composition and size,^{3,4} making it important to determine structural characteristics and physical properties of these particles so they can be used in practical applications. In the more microscopic world of small ultrafine particles, experiments to measure properties (such as thermodynamic properties) of these particles become very difficult. Fortunately, this is precisely the regime where computational chemistry is ideal for performing this analysis of the desired physical properties. Molecular dynamics (MD) simulation is an invaluable tool to study structural and dynamical details of polymer processes at the atomic or molecular level and to link these observations to experimentally accessible macroscopic properties of polymeric materials.^{5,6} Various MD simulations for polymers have been

used for exploring the properties,⁷⁻¹⁴ diffusion of small penetrants,^{15,16} and surface interactions¹⁷⁻²³ using periodic boundary conditions to simulate a bulk system. In contrast, we are most interested in nano-scale fine polymer particles to interpret the structure and properties of those particles distinguished from their bulk solid phase by the size and surface to volume ratio. In this article, we have carried out full classical MD simulation to study the atomistic details of the polyethylene (PE) particles with up to 60000 atoms under solvent free and vacuum condition.

METHODS

Hamiltonian

In this paper, we present calculations of some properties for nano-scale polymer particles generated with up to 60000 atoms using MD simulations. These simulations compute the momenta and coordinates of each atom in the system as a function of time by numerically integrating Hamilton's equations of motion using the molecular Hamiltonian written in Cartesian coordinates.^{24,25} The classical equations of motion are formulated using our geometric statement function approach²⁶ which reduces the number of mathematical operations required by a factor of ~ 60 over traditional approaches. These coupled equations are solved using novel symplectic integrators developed in our laboratory which conserve the volume of phase space and robustly allow integration for virtually any time scale.²⁷ As a simplification without loss of information of the polyethylene monomer, we collapsed the CH₂ and CH₃ groups into a single particle (bead) of mass $m = 14.5$ amu. By neglecting the internal structure of those groups, we reduce the number of equations of motion for the system and save a significant amount of computational time. In addition, it is reasonable to assume that high frequency modes of C-H stretch and bending are decoupled with

[†] This research is sponsored by the Division of Materials Sciences, Office of Basic Energy Sciences, U.S. Department of Energy under contract DE-AC05-96OR22464 with Lockheed-Martin Energy Research Corp.

the lower frequency vibrations and contribute little to thermal properties of the particles.²⁸ A classical molecular Hamiltonian for this model can be written in terms of the kinetic and potential energy of the system,

$$H = \sum_{i=1}^N \frac{p_i^2}{2m} + \sum_{i=1}^{N-1} V_{2b}(r_{i,i+1}) + \sum_{i=1}^{N-2} V_{3b}(\theta_{i,i+1,i+2}) + \sum_{i=1}^{N-3} V_{4b}(\tau_{i,i+1,i+2,i+3}) + \sum_{i=1}^{N-3} \sum_{j \geq i+3}^N V_{Nb}(r_{ij}), \quad (1)$$

where N is total number of atoms and p_i is the Cartesian momentum of the i th atom. The r , θ , and τ are the internal coordinates for the interatomic distance, the bending angle between three consecutive atoms, and the torsional angle between four consecutive atoms, respectively. The last term of the potential energy functions in eq 1 is the nonbonded two-body interaction ($j \geq i+3$). The potential functions and parameters used for the PE particles^{29,30} are given in Table I.

Modeling of Polymer Particles

A computational algorithm for generating and modeling polymer particles for our simulations was developed for constructing particles that are as similar as possible to the experimentally created polymer particles. This experimental technique was developed originally for probing single molecules liquid droplets.^{31,32} In the experiment, the refractive index obtained from the data analysis for micro and nano-scale particles is consistent with bulk (nominal) values and the level of agreement with Mie theory indicates that the generated particles are nearly perfect spheres.³³ In order to obtain initial conditions for nano-scale polymer particles, we have

developed an efficient method.^{34,35} In brief, the procedure starts by preparing a set of randomly coiled chains by propagating a classical trajectory with a perfectly planar all-*trans* zigzag initial conformation and randomly chosen momentum with a temperature of 300 K.³⁶⁻³⁸ The trajectory is terminated at 200 ps, and position and momenta of the chain are saved. By repeating this process, a desired set of randomly coiled chains is prepared. Six chains are selected randomly from the prepared sets and are placed along the Cartesian axis. Those chains are propelled at the appropriate amount of momentum to create a collision at the origin. The particle produced from this collision consists of the 6 chains is then annealed to a desired temperature and rotated through a randomly chosen set of angles in three dimensional space. Another set of six chains is then propelled at the particle to create another particle with 600 more atoms added in a symmetric but random orientation to build up the particle. This process is continued until the desired size is achieved for our study. Figure 1 illustrates the process to generate initial conditions for the different size of PE particles. After a desired particle size is obtained, classical trajectories were propagated for 50 ps above the melting point for bulk PE and then annealed until the temperature reached 10 K to find a steady state of the amorphous PE particles. Figure 2 shows PE particles of 60000 atoms with chain lengths of 100 beads.

We have also generated the PE particles with various chain lengths (50, 200, and 400 beads) based on the initial configurations of the generated amorphous PE with a chain length of 100 beads. To do this, we simply expand the space of the particle with a chain length of 100 beads by multiplying the initial configuration by two in Cartesian coordinates. Then, a new atom is inserted between the two atoms of the particles. Thus, the total number of atoms is doubled and the particle created consists of a chain length of 200 beads. For the particle with a chain length of 50 beads, the two, three, and four-body bonded interaction are simply turned off every 50 beads. Finally, classical trajectories are propagated with randomly chosen momenta until the density reaches 0.7 g cm^{-3} and annealed to a desired temperature. It is noted that the density for the particles is low ($\leq 0.05 \text{ g cm}^{-3}$) and temperature is very high ($\geq 1000 \text{ K}$) at a start of those trajectories, since the space of the original particle is expanded. Using this scheme, we can efficiently create large number of atoms with various

Table I. Potential parameters

Stretch	$V_{2b} = 1/2 \cdot k_r (r_{i,i+1} - r_0)^2$	
C-C	r_0 1.53 Å	k_r 2651 kJ mol ⁻¹
Bending	$V_{3b} = 1/2 \cdot k_\theta (\cos \theta_{i,i+1,i+2} - \cos \theta_0)^2$	
C-C-C	θ_0 113°	k_θ 130.1 kJ mol ⁻¹
Torsion	$V_{4b} = 8.77 + \alpha \cos \tau_{i,i+1,i+2,i+3} + \beta \cos^3 \tau_{i,i+1,i+2,i+3}$	
C-C-C-C	α -18.41 kJ mol ⁻¹	β 26.78 kJ mol ⁻¹
Nonbond	$V_{NB} = 4\epsilon [(\sigma/r_{ij})^{12} - (\sigma/r_{ij})^6]$	
CH ₂ ...CH ₂	ϵ 0.494 kJ mol ⁻¹	σ 3.98 Å

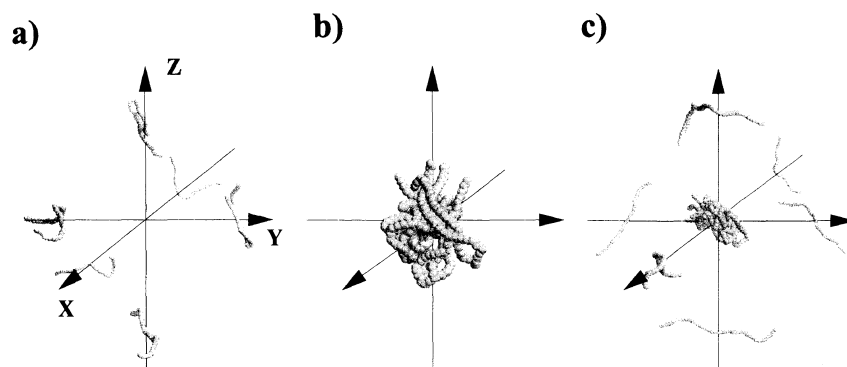


Figure 1. Creation of polyethylene particles for initial conditions: a) randomly coiled 6 chains with chain length of 100 beads, b) particle for 600 atoms with those 6 chains, and c) the rotated particles and a new set of 6 chains.

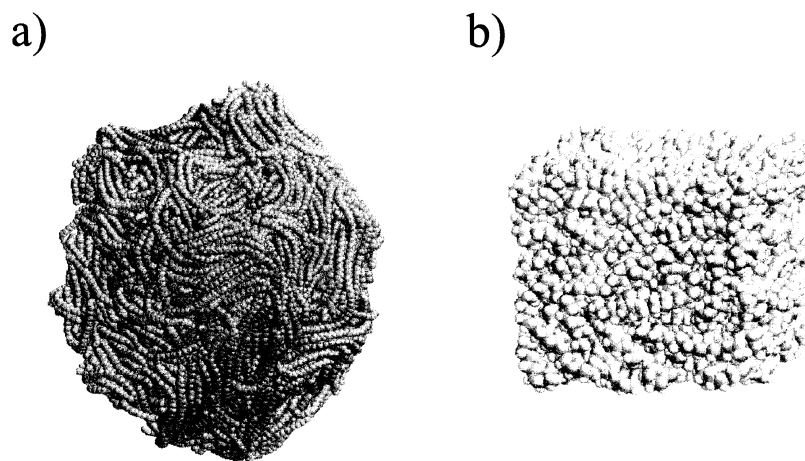


Figure 2. Polyethylene particle for 60000 atoms with chain length of 100 beads. The diameter of the drops for 60000 atoms is 12.5 nm. The diameter of the particle is the averaged value of distance from a center of mass to the surface atoms. Polyethylene bulk system b) has 9664 atoms with chain length of 100 CH₂ with hydrogen atoms in the length of 4.6 nm cubic cell.

chain lengths without propelling sets of 6 chains.

Modeling of Bulk System

Figure 2 also shows the PE bulk system in a cubic cell at the unit cell dimension of 4.6 nm. For creation of a polyethylene bulk system, a system consisting of 32 CH₂ chains with 100 C and 202 H atoms are placed in a cell, and the initial configuration of the system was optimized using molecular mechanics calculation.³⁹ With the initial conformation, MD simulations are propagated by applying an external force to the cell every 2 fs in order to pack the chains into the cell with the desired density. The density is calculated by using a cubic box with a dimension of 32 Å. The position of the box was randomly chosen in the cell, and then the number of the atoms in the box were found. The process is repeated 10 times, and the averaged density is monitored. The simulation is terminated when the density reaches 0.85 g cm⁻³ (bulk amorphous PE density).

We employ three-dimensional periodic boundary conditions to mimic the presence of an infinite bulk. The cell [Figure 2(b)] is surrounded by the identical cells; thus the atoms in the original cell can interact with all other atoms in those surrounded cells. Under the boundary conditions, classical trajectories are propagated for 10 ps. It is noted that we considered all atoms of PE polymer for the simulations of the bulk system in order to compare the computed structural conformations (*e.g.*, radial distribution) with X-ray and neutron scattering experiments. The radial distribution of the simulated bulk PE was in good agreement with the experimental data. Comparing the bulk system with the nano-scale spherical particles, we can study the conformational changes of the particles due to the size reduction and the shape.

Analysis

Average values of properties of the particles at a fixed temperature are obtained to examine dependence of the conformations and properties on temperature using the Nosé–Hoover chain (NHC) constant temperature molecular dynamics.⁴⁰ The initial configurations of the steady state of the amorphous PE particles are used at

a start of the NHC simulations; the initial values of the Cartesian momenta are given random orientation in phase space with magnitudes chosen so that the total kinetic energy is the equipartition theorem expectation value.⁴¹ The temperature of the particle, T , is calculated from,

$$\frac{3}{2} N k_{\text{B}} \langle T \rangle = \left\langle \sum_{i=1}^N \frac{p_i^2}{2m} \right\rangle \quad (2)$$

where k_{B} is the Boltzmann constant and N is the total number of atoms. Monitoring the temperature of the system, we found the system reaches the desired temperature during the first 10 ps. The reported characteristics of the particles are the averaged values calculated from the NHC trajectories in the range from 10 ps to 100 ps at the temperature.

In analyzing surface effects of ultra fine polymer particles, we calculated the surface area and volume using Connolly's contact-reentrant method.^{42,43} The contact-reentrant surface (molecular surface) uses a spherical probe which can trace molecular shape while in contact with the van der Waals surface. The van der Waals surface treats a CH₂ bead as a rigid hard sphere equal to the van der Waals radii, and the union of the spheres in the droplets is considered as the volume. The method provides a smooth surface by patching the space between the probe radius and the probed molecule. For our surface area and volume calculations, the van der Waals radius for the PE droplets is set at 1.89 Å for CH₂ beads and the probe radius at 1.4 Å to mimic H₂O molecule. Using the molecular surface, we also computed a fractal dimension, D , to show how irregular the PE droplets are (surface roughness). The value can be calculated by

$$D = 2 - \frac{d \log A_s}{d \log R_p} \quad (3)$$

where A_s and R_p are the molecular surface area and probe radius, respectively. The fractal dimension determined by the slope has values in the range 2–3; the lower limit corresponds to a smooth surface and the upper limits to a space-filled surface.

Experimental measurements of a melting point (T_m)

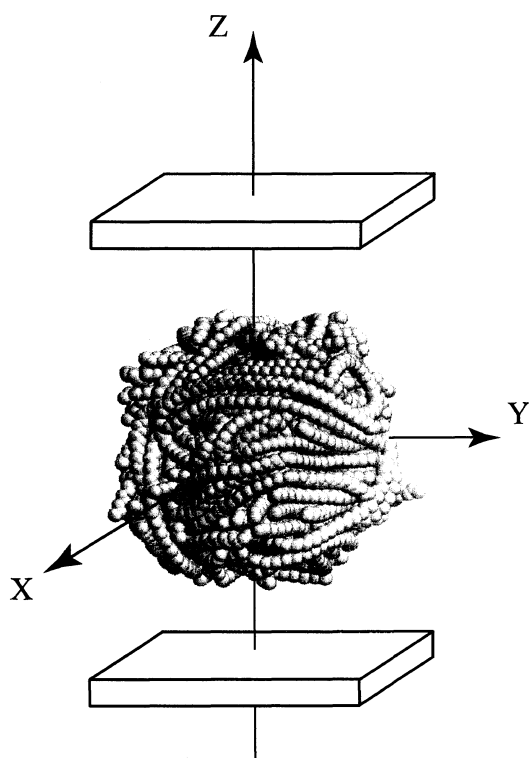


Figure 3. Schematic of the geometry for stress-strain MD simulations.

and glass transition temperature (T_g) are crucial properties that can be used to assess the physical state of a polymer. In our simulations, the melting point and the glass transition temperature can be obtained by calculating total energy and molecular volume of a system as a function of temperature. For a transition from the amorphous (solid) to the melt phase (liquid) and a glass-rubber transition, the volume increases owing to conformational disorder of the polymer droplets. Temperature and volume are calculated while annealing the drops gradually by scaling the momenta with a constant scaling factor. From least squares fits to molecular volume vs. temperature above and below the transition temperatures, we take the point where the extrapolated straight lines intersect, as T_m and T_g .

Mechanical Property: Compressive (Bulk) Modulus

It is of interest to study the behavior of polymer fine particles under an applied external force in order to investigate the deformation property and mechanical memory. One of the experimentally obtained values of those properties is known as Young's modulus which is a fundamental measure of the stiffness of a material. Numerous calculations have been performed for the mechanical property of bulk-like crystalline PE polymer using force field,⁷⁻¹² semiempirical,⁴⁴ *ab initio* calculation,^{45,46} and *ab initio* MD methods.^{47,48} In this study, we have calculated the compressive (bulk) modulus for the amorphous PE particles using MD with an external force as shown in Figure 3. At the start, a plate treated as a continuous wall is set at 10 Å from the closest atom of the particle in z coordinate (the distance from the origin to the plate is defined as L and the other plate is set at $-L$ in Cartesian coordinate.). The initial values

of the Cartesian momenta are chosen randomly in the amorphous particle to set initial temperature less than the melting point (200 K) and the system was fixed with zero center-of-mass position and velocity. The plates are moved 0.1 Å every 0.5 ps and the total energy for L was calculated every 0.5 ps. Young's modulus is defined,

$$\sigma = Y\varepsilon \quad (4)$$

where σ and ε represent the tensile stress and strain, respectively. In our calculation, the strain is the fractional change in dimension, $\varepsilon = (L_0 - L)/L_0$, and the stress is a force per unit area, $\sigma = F/\text{area}$. Since the external force is applied to the system, the particles start deforming, and the total energy is fluctuated. We define L_0 which gives the minimum total energy of the system. To find the *area* (πr_{ave}^2) of the particles, the particles are projected on the xy plane, and the distance of each atom from the origin is calculated at the L_0 . The distance r_{ave} can be approximately calculated from,

$$r_{\text{ave}} = \frac{\sum_{i=1}^N (x_i^2 + y_i^2)^{1/2}}{N} \quad (5)$$

The force applied to the particle is calculated from,

$$F = \frac{dE_T}{dL} \quad (6)$$

where E_T is the total energy of the system. By monitoring stress and strain, we obtain the compressive (bulk) modulus and yield point for the PE particles.

RESULTS AND DISCUSSION

Characteristics of Nano-Scale Polymer Particles

We modeled fine polymer particles which should closely correspond to the ones that can be experimentally created from a droplet generator that can efficiently generate nearly perfect spherical sub-micron particles of arbitrary composition. Using the molecular dynamics technique, PE particles with chain lengths of 100 beads generated with up to 60000 atoms have almost a spherical shape (asymmetry parameter ≈ -0.1 at a temperature of 10 K) as shown in Figure 2, in good agreement with our experimental results. To interpret properties of the polymer fine particles differing from their bulk solid phase, we first counted the surface atoms using a three-dimensional grid method in Cartesian coordinates and the ratio of the surface atoms to the total number of atoms are obtained (the diameter is the average value of distance from a center of mass to the surface atoms). Since the smaller sized particles have more surface atoms than the larger ones, a decrease of the diameter increases the ratio as shown in Table II. The large ratio of surface atoms to the total number of atoms provides reduction of the nonbonded interactions for the surface layer; hence the cohesive energy is dramatically dependent on the size.

The surface area and volume are calculated using the contact-reentrant surface method with a probe radii, $R_p = 1.4$ Å. The large proportional surface area defined by $S_{\text{ratio}} = (\text{surface area})/(\text{volume})$ leads to large surface free energy, which is described by per unit of surface area (J nm^{-2}). The S_{ratio} of the particles is large compared

Table II. Characteristics in fine polymer particles

No. of atoms	Diameter	Ratio of surface atoms	Area ^a	Volume ^a	S_{ration}	Fractal dimension ^b /nm ⁻¹
	nm					
3000	4.7	72%	152	67	2.27	2.14
6000	5.6	70%	257	138	1.86	2.15
9000	6.4	69%	346	209	1.65	2.16
12000	7.0	67%	443	279	1.55	2.16
18000	8.1	65%	610	419	1.46	2.19
24000	9.0	64%	814	564	1.44	2.21
30000	9.7	62%	955	706	1.35	2.21
60000	12.4	60%	1879	1424	1.32	2.26

^aThe probe radius is set at 1.4 Å. ^bThe probe radius is in the range from 2.0 to 3.5 Å.

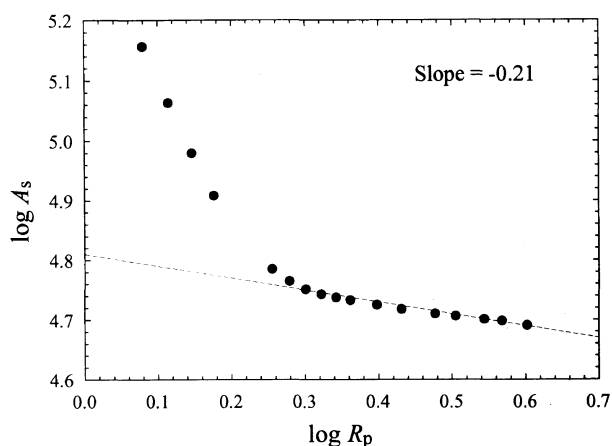


Figure 4. Dependence of molecular surface area, A_s , on probes with radii, R_p , of 1.4 to 4 Å for polyethylene particle of 30000 atoms with chain length of 100 beads. The slope of straight line for $\log A_s$ vs. $\log R_p$ with the least squares fit is 0.21. The value of fractal dimension is evaluated for probe radii in the range of 2.0 to 4.0 Å.

with that of the bulk so that the surface area and surface free energy are large. The surface of the particles is also characterized by the fractal dimension which describes a degree of irregularity of a surface.^{42,49,50} Figure 4 shows dependence of surface area on probe radii for the PE particle of 30000 atoms with a chain length of 100 beads. The slope is calculated for the probes in the range of 2.0 and 4.0 Å. The values of D are smaller for the particles than the value of the bulk ($D=2.72$). This indicates that the surface is irregular and has many cavities which may introduce unique (catalytic or interpenetrating) properties of polymer fine particles. Although a smaller probe can provide more detail of the polymer surface than the larger, the fractal dimension for the probe in the range of 1.4 and 2.0 is out of the physical limit. As the size of the probe decreases, the area of the surface rapidly increases. Since the smaller probe penetrates the cavities on the surface, the values of the area and surface are strongly dependent on the probe. This predicts that nano-scale polymer particles are loosely packed and can show dynamical flexibility (*e.g.*, compressive modulus of the particles is much smaller than that of the bulk system). The free volume (cavities) and molecular packing can be important in a diffusion rate of a small molecule trapped in the particles.⁵¹ The structural characteristics of the PE particles up to 60000 atoms with a chain length of 100

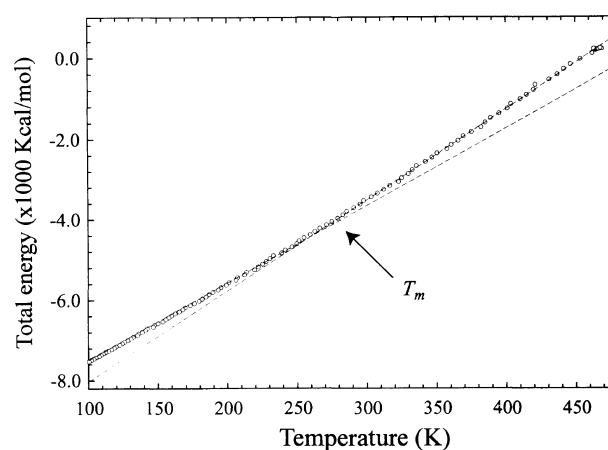


Figure 5. The total energy as a function of temperature while annealing the polyethylene particle which consists of 30000 atoms with a chain length of 100 beads. The open circles are the total energy calculated from MD simulations and dashed lines show the least squares fit. The intersection of extrapolated straight lines corresponds to the melting point, $T_m=258$ K. The slopes of the lines are 225900 and 192100 cal mol⁻¹ K⁻¹, respectively.

beads are shown in Table II.

Thermal Analysis

Thermal analysis provides a great deal of practical and important information about the molecular and materials world relating to equations of state, critical points and the other thermodynamics quantities. For our study of thermodynamic properties of nano-scale polymer particles, we have calculated temperature, volume, and total energy in the process of annealing the system by scaling the momenta at a constant rate. To determine the appropriate annealing schedule,³⁴ we have examined the melting point and glass transition temperature for the particle of 12000 atoms with a chain length of 100 beads for different rates in the range from 1.7 K ps⁻¹ to 29.5 K ps⁻¹. The transition temperatures were found to be rather insensitive (within the error of ± 5 K) to annealing rates slower than 6.0 K ps⁻¹. In all subsequent simulations, we set the annealing rate at approximately 2.5 K ps⁻¹ so that the particle is thermally equilibrated for each sampling point. Computing the straight lines of total energy of the system or molecular volume vs. temperature with a least square fit, we take the points where those extrapolated straight lines meet, as the melting point, T_m , and the glass transition temperature, T_g . Figure 5 shows dependence of total energy of the

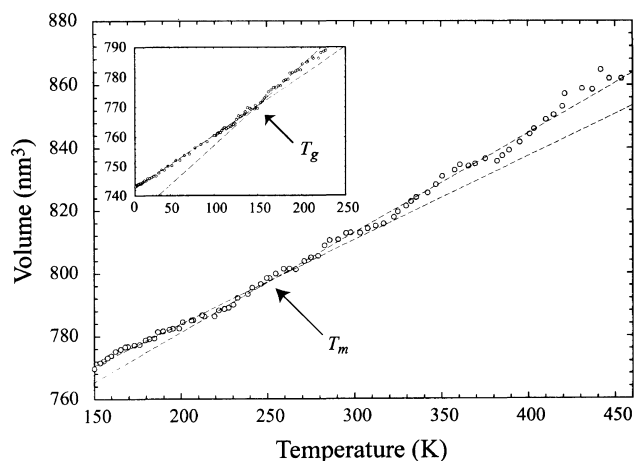


Figure 6. The molecular volume as a function of temperature while annealing the polyethylene particle which consists of 30000 atoms with a chain length of 100 beads. The open circles are the volume calculated from MD simulations and dashed lines show the least square fit. The intersection of extrapolated straight lines corresponds to the melting point, $T_m = 260$ K. The insert shows the glass transition temperature, $T_g = 152$ K.

system on temperature for the PE particle of 30000 atoms with a chain length of 100 beads. The slopes provide the constant pressure heat capacity, C_p , above and below the melting point. Figure 6 shows molecular volume as a function of temperature. The melting points calculated from molecular volume for the different size of the PE particles with various chain lengths are close to those values calculated from total energy within an error of ± 10 K. The agreement in the melting points supports our hypothesis that it is possible to extract the melting point for a variety of nano-scale polymer particles from MD simulations. We have reported the melting point from the simulation of energy vs. temperature instead of volume vs. temperature, since it is more straightforward to compute the linear lines from energy vs. temperature than from volume vs. temperature. Table III summarizes thermal properties of the PE particles with respect to size and various chain lengths.

Figure 7 shows dependence of melting point and glass transition temperature on the diameter of the particles. The dramatic reduction of the melting point for the fine polymer particles is an example of surface effects and shows the importance of size. Since the large ratio of surface atoms to the total number leads to a significant reduction of the non-bonded interactions, the melting point decreases with decrease of the total number of atoms. Figure 8 shows the effect of chain length on transition temperatures. A strong dependence of the melting point and the glass transition temperature on chain length is attributed to molecular weight and non-bonded energy of each chain.

Conformations

Figure 9 shows radial distribution functions for the PE particles of 12000, 30000, and 60000 atoms with a chain length of 100 beads at a temperature of 100 K. For the amorphous PE particles, the peak positions of the radial distributions are insensitive to the size in the diameter range 12.5 nm. By comparing the peak positions of the radial distributions of the particles with the bulk

Table III. Thermal properties of polyethylene particles

No. of atoms	Cohesive energy ^a kcal mol ⁻¹	T_m	T_g	C_p /cal mol ⁻¹ K ⁻¹	
		K	K	$T \leq T_m$	$T \geq T_m$
Chain length of 100 beads					
3000	3010	218	111	6.37	7.57
6000	6510	234	134	6.50	7.70
9000	10170	242	131	6.44	7.22
12000	13900	242	157	6.47	7.24
18000	23900	249	155	6.44	7.66
24000	32000	254	154	6.45	7.95
30000	41170	258	152	6.40	7.53
60000	82950	266	161	6.65	7.80
Chain length of 50 beads					
6000	7510	186	73	6.20	7.23
12000	15300	218	110	6.37	7.74
18000	25300	220	117	6.37	7.96
24000	34400	232	125	6.53	7.83
Chain length of 200 beads					
6000	5738	285	152	6.37	8.02
12000	10020	317	162	6.76	7.73
18000	18800	332	168	6.81	8.32
24000	25200	345	172	7.03	8.22
Chain length of 400 beads					
6000	4059	304	165	6.22	7.57
12000	9580	323	166	6.42	8.00
Chain length of 1000 beads					
6000	3112	331	169	6.22	8.17
12000	6186	349	171	6.96	8.35
Bulk ^b					
	9073	414	195	5.19	7.67

^aThe values are calculated from NHC simulations at 10 K.

^bCubic boundary conditions were used with a box length of 4.6 nm. The values of C_p are from ref 58 at 300 K and 400 K.

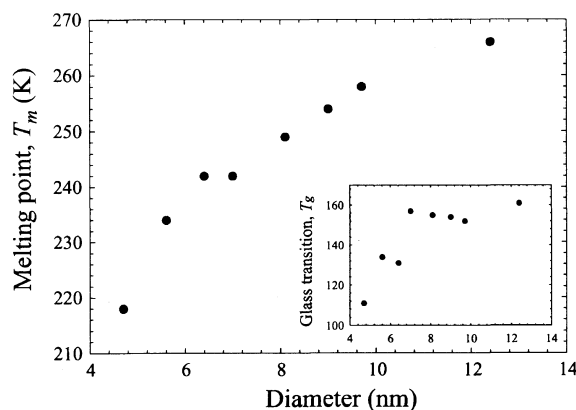


Figure 7. Dependence of the melting points on diameter for PE particles with a chain length of 100 beads.

system, it is clear that the peak around 3.15 \AA corresponding to *gauche* configuration is very small for the particles. The reduction of *gauche* configuration in the radial distributions is believed to be due to alignments

of the chains on the surface. In our previous study, we monitored the averaged end-to-end distances of the surface- and inner-chains for the particle of 12000 atoms with a chain length of 100 beads. The average end-to-end distance of the surface chains is longer than that of the inner chains, and the inner chains have more *gauche* configurations than the surface.³⁴

Several simulations have been applied to study the morphology of single or multiple chains with different chain lengths.^{21,36–38,52} Since the surface chains of the PE nano-particles tend to straighten and align at temperatures below the melting point, the preferential

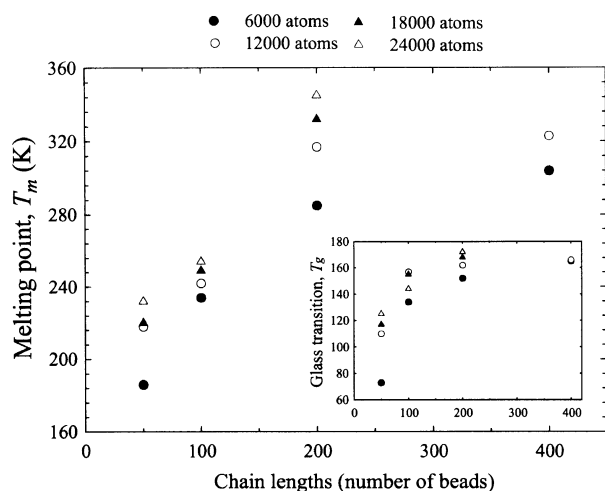


Figure 8. Dependence of the melting points on chain lengths.

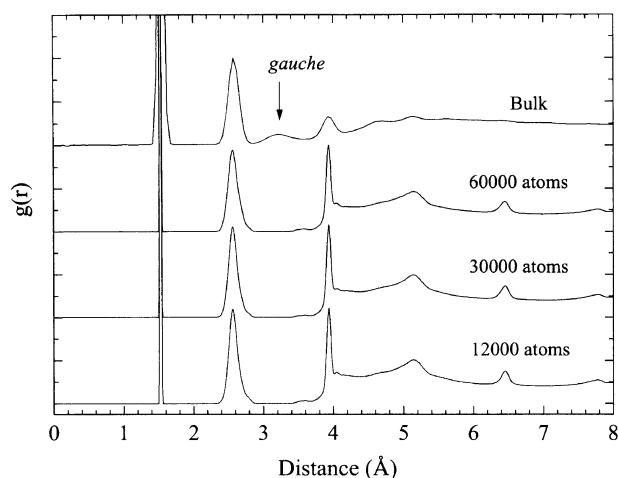


Figure 9. Dependence of the radial distributions on size of polyethylene particles with a chain length of 100 beads. Those distributions are calculated from NHC constant temperature MD simulations. The three peaks are 1.54, 2.57, and 3.94 Å corresponding to the distance of C_i-C_{i+1} , $C_i \cdots C_{i+2}$ and $C_i \cdots C_{i+3}$ (*trans*), respectively.

morphology for the small PE particle with a long chain length is a rod-like shape. This mechanism was also observed by Liu and Muthukumar in the simulations of polymer crystallization.²¹ This stretching of the chains leads to reduction of the cohesive energy and an increase in volume. Studies on the effect of a chain length show that the particles with the shortest chain length (50 beads) have the most spherical shape.

Mechanical Properties

The compressive modulus, which is quantified by the relation between stress and strain, are investigated for the PE particles by applying an external force in the MD simulations. Figure 10 is a plot of the stress as a function of strain for a PE particle consisting of 12000 beads with a chain length of 100 beads. The slope calculated for the proportional range gives a modulus for compression of the polymer nano-particles. It is known that values of the tensile modulus of bulk polyethylene are between 210 and 340 GPa.⁵³ In general, the compressive modulus is higher than the tensile modulus.^{54,55} In addition, the bulk and tensile strength or yield point are usually much smaller than the modulus for a thermoplastic such as polyethylene. In the MD study of the nano-particles, we have observed a compressive modulus that is orders of magnitude smaller than the bulk values and the yield point is much larger than the modulus. The stress-strain curve actually looks more like a curve for an elastomer. However, the initial deformation caused by the compression (that which gives the modulus) is not

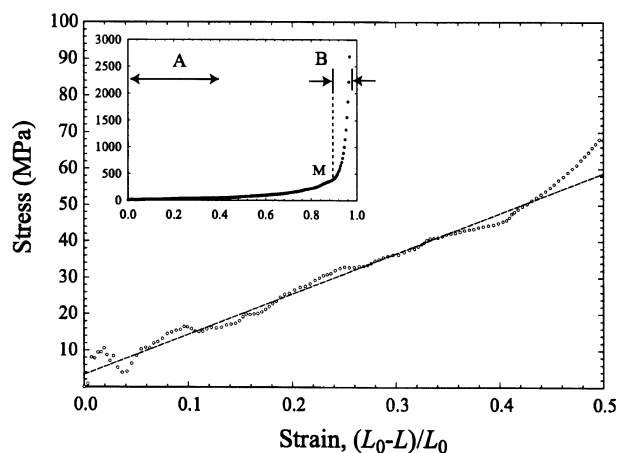


Figure 10. Stress-strain behavior for the PE particle of 12000 atoms with a chain length of 100 beads. The yield point is indicated at point M. The region of non-reversible deformation caused by the compression is labeled A: the region of reversible deformation is labeled B. The slopes calculated in the strain range from 0 to 0.4 (region A) and from 0.86 to 0.97 (region B) are 111 MPa and 85 GPa, respectively.

Table IV. Mechanical properties in fine PE particles^a

No. of atoms	Compressive modulus (A)		Compressive strength ^b	Compressive modulus (B)
	MPa	MPa	Mpa	GPa
3000	68	288		46
6000	86	324		63
9000	88	327		67
12000	111	400		85

^aThe modulus are calculated from the region of non-reversible and reversible deformation (see Figure 9, label A and B). ^bThe strength is obtained at the point, M.

reversible (region A in Figure 10). What occurs during this phase is the deformation of a spherical particle to an oblate top. This structure is stable but it lies at a slightly higher energy than that for a spherical particle. Thus, the modulus for compression in this region is actually more a measure of the force required to deform the spherical polymer particle into an oblate top (pancake-like structure^{3,56}). Further deformation tends to be reversible up to the point of rupture (region B in Figure 10). This deformation is actually more closely related to the bulk modulus since the stress is due to the cohesive energy and not a microstructure. This leads to a yield point that is significantly larger than the modulus. Table V shows the dependence of the mechanical properties of PE particles on size.

CONCLUSIONS

In this study of ultra fine polymer particles using molecular dynamics simulations, we have used a previously developed method for modeling nano-size polymer particles with various chain length and analyzed the thermal and mechanical properties of the particles generated with up to 60000 atoms. It is found that surface effects provide interesting properties that are different from those of the bulk polymer system. In particular, the melting point and glass transition temperature were found to be dramatically dependent on the size of the polymer particles. This study also demonstrated that the nano-scale PE particles have dynamical flexibility and behave like an elastomer. The result is quantified by the fractal dimension and compressive modulus. We are currently extending this model and methodology to larger size particles and other types of polymer systems to study the interfacial tension between incompatible polymers, shear flow effects, and thermal properties of blended polymer particles.⁵⁷ The molecular dynamics simulations used here should provide useful insights to explain and predict the properties and behavior of ultra fine polymer particles to be used in future new materials and devices.

Acknowledgments. K. F. is supported by the Post-doctoral Research Associates Program administered jointly by Oak Ridge National Laboratory and the Oak Ridge Institute for Science and Education.

REFERENCES

1. N. Ichinose, Y. Ozaki, and S. Kashu, "Superfine Particle Technology," Springer-Verlag, London, 1992.
2. C. Hayashi, R. Uyeda, and A. Tasaki, "Ultra-Fine Particles Technology," Noyes, New Jersey, 1997.
3. C.-Y. Kung, M. D. Barnes, B. G. Sumpter, D. W. Noid, and J. U. Otaigbe, *Polym. Prepr., Am. Chem. Soc., Div. Polym. Chem.*, **39**, 610 (1998).
4. M. D. Barnes, C.-Y. Kung, N. Lermer, K. Fukui, B. G. Sumpter, and D. W. Noid, *Opt. Lett.*, **24**, 121 (1999).
5. D. N. Theodorou and U. W. Suter, *Macromolecules*, **18**, 1467 (1985).
6. D. N. Theodorou and U. W. Suter, *Macromolecules*, **19**, 139 (1986).
7. D. Brown and J. H. R. Clarke, *Macromolecules*, **24**, 2075 (1991).
8. H. A. S. Argon and U. W. Suter, *Macromolecules*, **26**, 1097 (1993).
9. C. F. Fan, T. Cagin, Z. M. Chen, and K. A. Smith, *Macromolecules*, **27**, 2383 (1994).
10. C. F. Fan and S. L. Hsu, *Macromolecules*, **25**, 266 (1992).

11. Z. Sun, R. J. Morgan, and D. N. Lewis, *Polymer*, **33**, 2179 (1991).
12. D. W. Noid and G. A. Pfeffer, *J. Polym. Sci., Part B*, **27**, 2321 (1989).
13. Y. Jin and R. H. Boyd, *J. Chem. Phys.*, **108**, 9912 (1998).
14. A. Koike, *Macromolecules*, **31**, 4605 (1998).
15. M. Fukuda and S. Kuwajima, *J. Chem. Phys.*, **107**, 2149 (1997).
16. D. N. Theodorou, *Macromolecules*, **22**, 4578 (1989).
17. J. Hautman and M. L. Klein, *Phys. Rev. Lett.*, **67**, 1763 (1991).
18. W. Mar and M. Klein, *J. Phys. Condensed Matter*, **6**, A381 (1994).
19. D. N. Theodorou, *J. Am. Chem. Soc.*, **22**, 4578 (1989).
20. X. Yang and X. Mao, *Comput. Theor. Polym. Sci.*, **7**, 81 (1997).
21. C. Liu and M. Muthukumar, *J. Chem. Phys.*, **103**, 9053 (1995).
22. Y. Zhan and W. L. Mattice, *Macromolecules*, **27**, 7056 (1994).
23. D. He, D. H. Reneker, and W. L. Mattice, *Comput. Theor. Polym. Sci.*, **7**, 19 (1997).
24. M. L. Klein, *Annu. Rev. Phys. Chem.*, **36**, 525 (1985).
25. W. G. Hoover, *Annu. Rev. Phys. Chem.*, **34**, 103 (1983).
26. D. W. Noid, B. G. Sumpter, B. Wunderlich, and G. A. Pfeffer, *J. Comp. Chem.*, **11**, 236 (1990).
27. S. K. Gray, D. W. Noid, and B. G. Sumpter, *J. Chem. Phys.*, **101**, 4062 (1994).
28. S. N. Kreitmeier, G. L. Liang, D. W. Noid, and B. G. Sumpter, *J. Thermal Anal.*, **46**, 853 (1966).
29. B. G. Sumpter, D. W. Noid, and B. Wunderlich, *J. Chem. Phys.*, **93**, 6875 (1990).
30. R. H. Boyd and S.M. Breittling, *Macromolecules*, **7**, 855 (1974).
31. C.-Y. Kung, M. D. Barnes, N. Lermer, W. B. Whitten, and J. M. Ramsey, *Anal. Chem.*, **70**, 658 (1998).
32. M. D. Barnes, N. Lermer, C.-Y. Kung, W. B. Whitten, and J. M. Ramsey, *Optics Lett.*, **22**, 1265 (1997).
33. M. D. Barnes, N. Lermer, W. B. Whitten, and J. M. Ramsey, *Rev. Sci. Instruments*, **68**, 2287 (1997).
34. K. Fukui, B. G. Sumpter, M. D. Barnes, D. W. Noid, and J. U. Otaigbe, *Macromol. Theory Simul.*, **8**, 38 (1999).
35. K. Fukui, B. K., Sumpter, M. D., Barnes, D. W. Noid, and J. U. Otaigbe, *Comput. Theor. Polym. Sci.*, in press.
36. G. Tanaka and W. L. Mattice, *Macromolecules*, **28**, 1049 (1995).
37. A. Michel and S. Kreitmer, *Comput. Theor. Polym. Sci.*, **7**, 113 (1997).
38. T. A. Kacassalis and P. R. Sundarajan, *Macromolecules*, **26**, 4144 (1993).
39. U. Burkert, N. L. Allinger, "Molecular Mechanics," American Chemical Society, Washington, D.C., 1982.
40. G. J. Martyna, M. L. Klein, and M. Tuckerman, *J. Chem. Phys.*, **97**, 2635 (1992).
41. K. Fukui, J. I. Cline, and J. H. Frederick, *J. Chem. Phys.*, **107**, 4551 (1997).
42. M. L. Connolly, *J. Am. Chem. Soc.*, **107**, 1118 (1993).
43. J. Doucet and J. Weber, "Computer-Aided Molecular Design: Theory and Applications," Academic Press Inc., San Diego, 1996.
44. T. Hor, W. Wade Adams, R. Pachter, and P. Haaland, *Polymer*, **34**, 2481 (1993).
45. B. Crist and P. G. Herena, *J. Polym. Sci., Part B, Polym. Phys.*, **34**, 449 (1996).
46. S. Suhai, *J. Polym. Sci., Polym. Phys. Ed.*, **21**, 1341 (1983).
47. R. J. Meier, *Macromolecules*, **26**, 4376 (1993).
48. J. C. L. Hageman, R. J. Meier, M. Heinemann, and R. A. de Groot, *Macromolecules*, **30**, 5953 (1997).
49. M. Lewis and D. C. Rees, *Science*, **230**, 1163 (1985).
50. J.-H. Choi, H. Kim, and S. Lee, *J. Chem. Phys.*, **109**, 7001 (1998).
51. P. V. Krishna Pant and R. H. Boyd, *Macromolecules*, **26**, 679 (1993).
52. H. Noguchi and K. Yoshikawa, *J. Chem. Phys.*, **109**, 5070 (1998).
53. J. Shoemaker, T. Horn, P. Haaland, R. Pachter, and W. W. Adams, *Polymer*, **33**, 3351 (1992).
54. L. E. Nielsen, "Mechanical Properties of Polymers and Composites," Marcel Dekker, Inc., New York, N.Y., 1974.
55. D. Porte, "Group Interaction Modelling of Polymer Properties," Marcel Dekker, Inc., New York, N.Y., 1995.
56. K. Fukui, B. G. Sumpter, C.-Y. Kung, M. D. Barnes, and D. W. Noid, *Chem. Phys.*, in press.
57. K. Fukui, B. G. Sumpter, M. D. Barnes, and D. W. Noid, in preparation.
58. N. Karasawa, S. Dasgupta, and W. A. Goddard, III, *J. Phys. Chem.*, **95**, 2260 (1991).